

3.0 Collisional-radiative models for beam attenuation and emission

3.1 Introduction

In this chapter we discuss the formulation and computational implementation of the bundled-nS deuterium beam model within the context of ADAS. The bundled-nSL helium beam model is also presented in a similar manner. It should be noted that the bundled-nS model was originally written in FORTRAN by Burgess and Summers[37] and was later modified by Spence[19]. In this work our main contribution to the bundled-nS model has been the optimising and validation of the program. Then we deployed it to model the attenuation and emission associated with the neutral deuterium beams at JET, see chapter 5.0. The bundled-nSL model was extensively developed during the course of this work for application to helium beams, although the code had its origin in an existing program designed to model the excited population structure of atoms in an astrophysical plasma[43]. The bundled-nSL is also written in FORTRAN. We have also developed interactive programs which interrogate and archive the output from each of these collisional-radiative models. The details of these programs are also discussed in this chapter.

3.2 The bundled-nS model for a deuterium beam

The bundled-nS model evaluates the excited population structure of neutral deuterium. The model is a very many n-shell treatment, in which the populations of a representative set of principal quantum shells are calculated since matrix condensation techniques are used to render the problem tractable[37]. Due to the near energy degeneracy of the l-substates of deuterium, the bundled-nS approximation, in even low density tokamak plasmas, suffices. Even in circumstances, where the degeneracy is partially removed (for example by the motional Stark perturbation), to a good approximation the population of the sub-states for a given n are statistical at tokamak densities. Our model is general in that the deuterium atoms can either be in thermal plasma, which may possibly be traversed by a neutral beam, or be the main constituents of a beam. In the case of deuterium atoms in a thermal plasma, the excited population structure and collisional-radiative recombination and ionisation coefficients are evaluated. In the present work we are concerned with deuterium

atoms in a beam, therefore the quantities of interest include only the excited population structure and the collisional-radiative ionisation coefficients. The effective ionisation coefficient, as mentioned earlier, represents the rate at which the beam atoms are ionised as the beam traverses the plasma and is commonly referred to as the effective beam stopping coefficient.

The statistical balance equations of the bundled-nS model include all the processes which contribute to populating and depopulating each principal quantum shell. These take the form shown below.

$$\begin{aligned}
v_b \frac{dN_i}{dx} = & \sum_{i' > i} \left(A_{i' \rightarrow i} + U(\nu) B_{i' \rightarrow i} + n_e q_{i' \rightarrow i}^e + n_p q_{i' \rightarrow i}^p + n^{(imp)} q_{i' \rightarrow i}^{(imp)} \right) N_{i'} + \\
& \sum_{i'' < i} \left(U(\nu) B_{i'' \rightarrow i} + n_e q_{i'' \rightarrow i}^e + n_p q_{i'' \rightarrow i}^p + n^{(imp)} q_{i'' \rightarrow i}^{(imp)} \right) N_{i''} + \\
& \left(\alpha_i^{RR} + \frac{n_b}{n_e} \alpha_i^{CX} + \int U(\nu) B_{k \rightarrow i} dk + \alpha_i^{(3)} n_e \right) n_e n_+ - \\
& \sum_{i' < i} \left(A_{i \rightarrow i'} + U(\nu) B_{i \rightarrow i'} + n_e q_{i \rightarrow i'}^e + n_p q_{i \rightarrow i'}^p + n^{(imp)} q_{i \rightarrow i'}^{(imp)} \right) N_i - \\
& \sum_{i' > i} \left(U(\nu) B_{i \rightarrow i'} + n_e q_{i \rightarrow i'}^e + n_p q_{i \rightarrow i'}^p + n^{(imp)} q_{i \rightarrow i'}^{(imp)} \right) N_i - \\
& \left(n_e q_{i \rightarrow \infty}^e + n_p q_{i \rightarrow \infty}^p + n_p q_{i \rightarrow \infty}^p + n^{(imp)} q_{i \rightarrow \infty}^{(imp)} + \int U(\nu) B_{i \rightarrow k} dk \right) N_i
\end{aligned} \tag{3.1}$$

for $i = 1, 2, 3, \dots$

Note the presence of a radiation field. This is viewed here as a possible external radiation field penetrating the plasma. Although the external radiation field on the population structure is treated correctly in atomic terms it is actually for the present beam studies an artificial device for population modification. This is discussed in section 3.2.5. There is no actual external radiation field present in our JET studies. $U(\nu)B_{i \rightarrow i'}$ corresponds to the contribution due to photo-excitation ($i' > i$) and stimulated emission ($i' < i$). The quantity $\int U(\nu)B_{k \rightarrow i} dk$ is the contribution due to stimulated recombination and $\int U(\nu)B_{i \rightarrow k} dk$ is the photo ionisation rate. The influence of plasma impurities are also included in the statistical balance equations. The protons¹ contained in the plasma are treated as special plasma species while the

¹ We use the term 'protons' to refer to any of the isotopes of fully stripped hydrogen.

remaining ions are treated as ‘impurities’. The symbol $n^{(imp)}$ represents the total effective impurity density. In general several impurity species may be involved in collisionally inducing transitions. If we let the set of impurity charges and fractions be $\{z_{0i}^{(imp)}, f_i^{(imp)}; i=1,..I\}$. Then the total effective impurity density and the effective charge Z_{eff} , as evaluated by the bundled-nS model is,

$$n^{(imp)} = (n_e - n_p) / \left(\sum_{i=1}^I z_{0i}^{(imp)} f_i^{(imp)} \right) \quad 3.2$$

$$Z_{eff} = \left(n_p + n^{(imp)} \sum_{i=1}^I (z_{0i}^{(imp)})^2 f_i^{(imp)} \right) / n_e \quad 3.3$$

and the number density of each individual impurity ion is simply,

$$n_i^{(imp)} = n^{(imp)} f_i^{(imp)} \quad 3.4$$

In the case of a single impurity, which is frequently used as an effective impurity, it is convenient to alter the definition. The effective charge for a single impurity and its number density is now evaluated as,

$$z_0^{(imp)} = (Z_{eff} n_e - n_p) / (n_e - n_p) \quad 3.5$$

$$n^{(imp)} = (n_e - n_p) / z_0^{(imp)} \quad 3.6$$

The bundled-nS model employs a wide range of approximate methods to evaluate the rate coefficients associated with the atomic processes which are included in the statistical balance equations. For convenience it is assumed that the electron and ion temperature are identical. We should point out that the beam atoms are in a purely ionising regime, therefore it is unnecessary to include recombining process such as radiative recombination (α^{RR}) and charge exchange (α^{CX}). These processes have only been included due to the general nature of the model. The program also access a collection of databases which contain more refined atomic data which is used to substitute the approximate methods where ever possible.

In the following sub-sections we briefly summarise the approximate methods and indicate the extent to which fundamental atomic data is used. A detailed account of the former is given by Spence[19]. We also outline the method which is adopted to solve the statistical balance equations.

3.2.1 Radiative atomic processes

We begin by first considering the spontaneous emission coefficient, which describes the rate at which an electron naturally decays from the upper level n to the lower level n' , this is calculated using the expression,

$$A_{n \rightarrow n'} = \left(\frac{16\alpha^4 c}{3\sqrt{3}\pi a_0} \right) \frac{z_0^4 g_{n,n'}^I}{n^3 n' (n^2 - n'^2)} \quad 3.7$$

where $g_{n,n'}^I$ is the bound-bound Gaunt factor[37], α is the fine structure constant, a_0 is the first Bohr orbit radius and z_0 is the nuclear charge of the beam atom. The spontaneous emission coefficient is then used to obtain expressions for the stimulated emission and photo-excitation coefficient. The Einstein B-values can be obtained using the following relations,

$$B_{n \rightarrow n'} = A_{n \rightarrow n'} \left/ \frac{8\pi}{c^3} h\nu^3 \right. \quad B_{n' \rightarrow n} = \frac{n^2}{n'^2} B_{n \rightarrow n'} \quad 3.8$$

Therefore the stimulated emission coefficient is,

$$U(\nu)B_{n \rightarrow n'} = \left(\frac{16\alpha^4 c}{3\sqrt{3}\pi a_0} \right) \frac{W z_0^4 g_{n,n'}^I}{n^3 n' (n^2 - n'^2)} \left[\exp\left(\frac{h\nu}{kT_r}\right) - 1 \right]^{-1} \quad 3.9$$

and the photo-excitation coefficient,

$$U(\nu)B_{n' \rightarrow n} = \left(\frac{16\alpha^4 c}{3\sqrt{3}\pi a_0} \right) \frac{W z_0^4 g_{n,n'}^I}{n n'^3 (n^2 - n'^2)} \left[\exp\left(\frac{h\nu}{kT_r}\right) - 1 \right]^{-1} \quad 3.10$$

where $U(\nu)$ is the energy density, T_r is the temperature of the radiation field and W is a dilution factor. The radiative recombination coefficient is evaluated using the following equation,

$$\alpha_n^r = 8 \left(\frac{\pi a_0^2 I_H}{k T_e} \right)^{3/2} \left(\frac{8 \alpha^4 c}{3 \sqrt{3} \pi a_0} \right) \frac{z_0^4}{n^3} \exp\left(I_n / k T_e \right) \int_{I_n / k T_e}^{\infty} \frac{g_{n,n}^{II} \exp(-x)}{x} dx \quad 3.11$$

where $g_{n,n}^{II}$ is the bound-free Gaunt factor[37] and $x = h\nu/kT_r$. The atomic process of photo-ionisation is now of interest . This coefficient is evaluated using the following expression,

$$\int U(\nu) B_{n \rightarrow \kappa} = \left(\frac{8 \alpha^4 c}{3 \sqrt{3} \pi a_0} \right) \frac{W z_0^4}{n^5} \int_{I_n / k T_r}^{\infty} \frac{g_{n,n}^{II}}{x [\exp(x) - 1]} dx \quad 3.12$$

and finally, the stimulated radiative recombination is given as,

$$\int U(\nu) B_{\kappa \rightarrow n} d\kappa = \frac{2^6}{3 \sqrt{3}} \left(\frac{\pi^{1/2} a_0^2 \alpha^4 c I_H^{3/2}}{k^{3/2} T_e^{3/2}} \right) \frac{W z_0^4}{n^3} \exp\left(I_n / k T_e \right) \int_{I_n / k T_r}^{\infty} \frac{g_{n,n}^{II} \exp(-T_r x / T_e)}{x [\exp(x) - 1]} dx \quad 3.13$$

3.2.2 Collisional atomic processes

There are three methods which the bundled-nS model can use to evaluate electron impact excitation rates. These include the method of Van Regemorter[44], the impact parameter approximation[37] and the prescription by Percival and Richards[45]. The method of Van Regemorter involves describing the electron excitation rate coefficients with effective P-factors. The electron impact excitation is then given as,

$$q_{n' \rightarrow n} = \frac{2^8}{3} \left(\frac{2 \sqrt{\pi} \alpha c a_0^2}{3} \right) \frac{n^5 n'^3}{(n^2 - n'^2)^4} \frac{g_{n,n'}^I}{z_0^2} \left(\frac{I_H}{k T_e} \right)^{3/2} \exp\left(-\frac{\Delta E_{n,n'}}{k T_e} \right) P\left(\frac{\Delta E_{n,n'}}{k T} \right) \quad 3.14$$

where $P(\Delta E_{n,n'}/kT_e)$ is the Van Regemorter P-factor and $\Delta E_{n,n'}$ is the transition energy between the levels n and n' . The corresponding de-excitation rate is then give as,

$$q_{n \rightarrow n'} = \frac{2^8}{3} \left(\frac{2\sqrt{\pi}\alpha c a_0^2}{3} \right) \frac{n^5 n'^3}{(n^2 - n'^2)^4} \frac{g_{n,n'}}{z_0^2} \left(\frac{I_H}{kT_e} \right)^{3/2} P \left(\frac{\Delta E_{n,n'}}{kT_e} \right) \quad 3.15$$

The basic expression to obtain the electron impact excitation cross-sections using the impact parameter method is,

$$\sigma_{n' \rightarrow n} = 2\pi \int_0^{\infty} P_{n' \rightarrow n} b db \quad 3.16$$

where b is the impact parameter and $P_{n' \rightarrow n}$ is the probability of the target electron being excited from the level n' , to the upper level n . As discussed in detail by Burgess and Summers[37], the probability $P_{n' \rightarrow n}$, can be evaluated using time dependent perturbation theory. However perturbation theory is only valid for weak coupling i.e. at large impact parameters. Therefore Burgess and Summers have derived expression according to whether the impact parameter is large enough to be considered for weak coupling or small enough for strong coupling. To avoid digressing we simply quote their results. In the case of weak coupling the excitation cross section is,

$$\sigma_{n' \rightarrow n} = \frac{I_H}{W_n} \left[8 \left(\frac{I_H}{\Delta E_{n,n'}} f_{n \rightarrow n'} \right) Y(\xi, \delta_0) \right] \pi a_0^2 \quad 3.17$$

and for strong coupling the excitation cross section described,

$$\sigma_{n' \rightarrow n} = \frac{I_H}{W_n} \left[8 \left(\frac{I_H}{\Delta E_{n,n'}} f_{n \rightarrow n'} \right) Y(\xi, \delta_1) + \frac{z}{a_0} R_1^c + 0.5 k_n k_{n'} (R_1^c)^2 \right] \pi a_0^2 \quad 3.18$$

A detailed description of each equation can be found in the [37]. Finally, the prescription of Percival and Richards[45], which is based on a combination of semi-classical methods and experimental data, yields the following expression,

$$\sigma_{n' \rightarrow n} = \frac{n^4 I_H \pi \alpha_0^2}{z_0^2 E} (ADL + FGH) \quad 3.19$$

the details of which can be found in [45]. The corresponding collisional de-excitation cross sections for both the impact parameter and the latter method are calculated using the principle of detailed balance.

If we now consider electron impact ionisation. There is only one approximate method which is available for use in the bundled-nS model. This is the Exchange Classical Impact Parameter (ECIP) method of Burgess[46]. The electron impact ionisation rate from the level denoted by the principal quantum number n is given as,

$$q_{n \rightarrow \infty} = (8\sqrt{\pi} \alpha c a_0^2) \left(\frac{I_H}{kT_e} \right)^{1/2} \frac{n^2}{z_0^2} \exp\left(-\frac{I_n}{kT_e}\right) \int_0^{\infty} G \exp(-\xi) d\xi \quad 3.20$$

where $\xi = (W_n - I_n) / kT_e$ and G is defined as,

$$G = \left[\left(\frac{W_n/I_n - 1}{W_n/I_n + 1} \right) - \frac{W_n/I_n}{(W_n/I_n + 1)^2} \ln\left(\frac{W_n}{I_n}\right) + \frac{1}{4} I^{IP}(W_n) \right] \quad 3.21$$

W_n is the initial energy of the incident electron and I^{IP} is the contribution due to impact parameter[37]. This expression is then used to obtain the three body recombination rate coefficient,

$$\alpha_n^{(3)} = 2^6 \pi^2 (\alpha c a_0^5) \left(\frac{I_H}{kT_e} \right)^2 \frac{n^4}{z_0^2} \int_0^{\infty} G \exp(-\xi) d\xi \quad 3.22$$

We now consider the methods which are employed to evaluate the ion impact excitation cross-sections. There are three different methods which are available for use. These include the impact parameter method[37], the semi-empirical formula of Lodge et. al.[47], and the two state approximation of Vainshtein et. al.[48]. The impact parameter method involves similar expressions to equations 3.17 and 3.18. A detailed description is given by Burgess and Summers[37]. The semi-empirical formula of Lodge et. al is based on a combination of semi-classical methods and experimental data. The resultant formula, for which the details can be found in [47] is,

$$\sigma_{n' \rightarrow n} = \frac{n^4 \pi a_0^2}{\bar{\epsilon}} (ADL + FGH) \quad 3.23$$

The two state approximation of Vainshtein et. al.[48] describes the behaviour of ion impact excitation with the following equation,

$$\sigma_{n' \rightarrow n} = 2\pi \left(\frac{\lambda}{v} \right) \exp(-2\sqrt{2\beta}) I(\beta) \quad 3.24$$

where $I(\beta)$ is calculated from a definite integral and λ is related to the oscillator strength[48]. The corresponding de-excitation cross sections for each method are also obtained using the principle of detailed balance. The last approximate method concerns ion impact ionisation. The bundled-nS model employs the binary encounter formula of Percival and Richards[49].

3.2.3 Beam thermal rate coefficients

The approximate methods employed by the bundled-nS model, with the exception of the method of Van Regemorter, evaluates the cross sections which described the behaviour of the collisional processes. However to assemble the statistical balance equations we must convert the cross sections into beam-thermal rate coefficients.

The collision between two particles in a thermal plasma is characterised by their relative velocity. The associated rate coefficient is defined as,

$$\langle v_r \sigma(v_r) \rangle = \int_{v_{\min}}^{\infty} \int_{v_{\min}}^{\infty} v_r f(v_p) f(v_t) \sigma(v_r) dv_p dv_t \quad 3.25$$

where v_r is the relative velocity between the target and the projectile. The quantities $f(v_t)$ and $f(v_p)$ are the corresponding velocity distributions for each particle. In the present work the projectiles are the beam atoms, which have a known velocity, and the target particles are the thermal ions contained in the plasma. Therefore the rate coefficient for the collision between the beam neutrals and target ions is,

$$\langle v_r \sigma \rangle = \int_{v_{\min}}^{\infty} v_r \sigma(v_r) f(v_t) dv_t \quad 3.26$$

The relative velocity is defined as $v_r = |v_p - v_t|$, which is expressed as,

$$v_r = |v_p - v_t| = \sqrt{v_p^2 + v_t^2 + 2v_p v_t \cos \vartheta} \quad 3.27$$

where ϑ is defined as the angle between the projectile and the target. The beam-thermal rate coefficient as evaluated in the bundled-nS model is then defined as,

$$\langle v_r \sigma(v_r) \rangle = \frac{1}{2} \int_0^{\pi} \int_{v_{\min}}^{\infty} v_r \sigma(v_r) f(v_t) \sin \vartheta dv_t d\vartheta \quad 3.28$$

It is of interest to point out that electrons in the plasma are moving with velocities much greater than that of the beam atoms. Therefore the rate coefficients associated with electron collisions are effectively independent of the beam velocity.

3.2.4 Fundamental atomic data

The supplementary data which is utilised by the bundled-nS model is now considered. There are three main databases which contain electron impact excitation, electron impact ionisation and ion-atom collision data respectively. If we first concern ourselves with electron impact excitation database. This database contains electron impact excitation coefficients which are stored in the form of effective

collision strengths[29]. The effective collision strengths are tabulated for transitions up to the n=5 shell. This data is periodically updated and is a combination of both theoretical and experimental data. During the course of this work the contents of the database was based on the calculations of Sampson and co-workers [50,51,52] and the data of Callaway[53]. This database also contains a compilation of spontaneous emission coefficients, the details of which can be found in [54]. Turning our attention to the electron impact ionisation database. This database contains Maxwell averaged rate coefficients which are periodically updated. The contents of the database during this work was based on the data reported by Bell et. al.[55]. The last database of concern, which is the largest by far, contains a wide range of ion-atom collision data. The database contains cross sections for charge exchange and ion impact ionisation from the ground and excited states up to the n=5 shell. Ion impact excitation data up to the n=5 shell is also included. The data is stored in the format of raw cross sections and encompasses the reactions mentioned for all the impurity species up to the first period. A detailed review of this database can be found in appendix A.

3.2.5 Method of solution

Due to the generalised nature of the bundled-nS model, rather than simply solving for the excited populations, an alternative approach is adopted. There are three basic driving mechanisms which are responsible for populating the excited levels of deuterium. These include charge exchange recombination, excitation from the ground state and recombination of free electrons. The model solves the statistical balance equations for each of the individual contributions associated with every principal quantum shell of interest. To obtain the individual contributions we start from the statistical balance equation written in matrix notation,

$$v_b \frac{dN_i}{dx} = n_e n_+ r_i - \sum_j C_{ij} N_j \quad 3.29$$

If we now re-write this expression in the form,

$$v_b \frac{dN_i}{dx} = n_e n_+ \mathfrak{R}_i + n_b n_+ \alpha_i^{CX} - \sum_j C_{ij} N_j \quad 3.30$$

where \mathfrak{R}_i is defined as,

$$\mathfrak{R}_i = \alpha_i^{RR} + n_e \alpha_i^{(3)} + \int U(v) B_{\kappa \rightarrow i} d\kappa \quad 3.31$$

We can now re-write expression 3.30 in terms of the quasi-static and non-equilibrium levels using the notation of chapter 2.0,

$$v_b \frac{dN_i}{dx} = n_e n_+ \mathfrak{R}_i + n_b n_+ \alpha_i^{CX} - \sum_{j>m} C_{ij} N_j^{eq} - \sum_{\sigma=1}^m C_{i\sigma} N_\sigma \quad 3.32$$

The expression for the equilibrium populations is,

$$N_j^{eq} = n_e n_+ R_j + n_b n_+ G_j + \sum_{\sigma=1}^m E^\sigma N_\sigma \quad 3.33$$

which distinguishes the different driving mechanisms,

$$R_j = \sum_{i>m} C_{ji}^{-1} \mathfrak{R}_i \quad 3.34$$

$$G_j = \sum_{i>m} C_{ji}^{-1} \alpha_i^{CX} \quad 3.35$$

$$E^\sigma = - \sum_{i>m} C_{ji}^{-1} C_{i\sigma} \quad 3.36$$

R_j , G_j , and E^σ are respectively the contributions which populate the excited levels of the beam atoms due to recombination, charge exchange and excitation from the non-equilibrium levels. For deuterium the number of non-equilibrium levels is one, therefore equation 3.33 now reads as,

$$N_j^{eq} = n_e n_+ R_j + n_b n_+ G_j + E^1 N_1 \quad 3.37$$

Rather than solving this equation directly it is more convenient to solve for the ‘ b_n -factors’ which are defined using the modified Saha-Boltzmann equation,

$$N_n = n_e n_+ 8 \left(\frac{\pi a_0^2 I_H}{kT_e} \right)^{3/2} n^2 \exp\left(\frac{I_n}{kT_e} \right) b_n \quad 3.38$$

The b_n factors describe the deviation from thermodynamic equilibrium at which they should be equal to a value of one. If we substitute the modified Saha-Boltzmann equation into equation 3.37 we arrive at,

$$b_n = F_{(n)}^1 \left(\frac{N_1}{n_+} \right) + F_{(n)}^2 + F_{(n)}^3 \left(\frac{n_b}{n_e} \right) \quad 3.39$$

where $F_{(n)}^1$, $F_{(n)}^2$ and $F_{(n)}^3$ are respectively the contributions which populate the level n due to excitation from the ground, recombination and charge exchange. The quantity n_b is the beam density and N_1 is the population of the ground state of the beam neutrals. In the present context our interest is with the $F_{(n)}^1$ quantity, since this gives the contribution which populates the excited levels of the beam atoms from their ground state.

We have a computational algorithm for distinguishing these contributions, we first fix the beam density to zero, this sets the contribution due to charge exchange to zero. We then apply a synthetic radiation field which depopulates the ground state due to the inclusion of photo-ionisation in the statistical balance equations. The $F_{(n)}^2$ recombination contribution can be calculated in isolation. If we then switch off the radiation field and keep the beam density as zero we can then evaluate the $F_{(n)}^1$ contribution. Finally, if the radiation field is set to zero and the beam density is not equally to zero the $F_{(n)}^3$ contribution can be calculated.

The quantities which are tabulated as output from the model include the b_n , $F_{(n)}^1$, $F_{(n)}^2$ and $F_{(n)}^3$ components. The solution of the Saha-Boltzmann equation in the form the $N_n/b_n \times n_+$ is also tabulated along with the effective beam stopping coefficients. Therefore the excited state population relative to the ground state can be obtained from the output since,

$$\frac{N_n}{N_1} = F_{(n)}^1 \left(\frac{N_n}{b_n n_+} \right) \quad 3.40$$

which allows us to define the effective beam emission coefficient for the transition $n \rightarrow n'$ as,

$$q_{n \rightarrow n'}^{BES} = \frac{A_{n \rightarrow n'}}{n_e} F_{(n)}^I \left(\frac{N_n}{b_n n_+} \right) \quad 3.41$$

where $A_{n \rightarrow n'}$ is the transition probability. The effective beam emission coefficient is the number of photons emitted per unit volume per second. The beam emission coefficient is employed to recover the neutral beam density from the D_α emission from the excited beam atoms in experimental analysis, see chapter 5.0.

3.3 The bundled-nISL model for a helium beam

The bundled-nISL model has been designed to operate in a similar manner to the bundled-nS model. The bundled-nISL models calculates the excited population structure of helium atoms either in a optically thin thermal plasma or in a mono-energetic beam penetrating into a plasma. It is an nl-spin resolved model which calculates the populations of the l-substates from the ground state up to an arbitrary principal quantum number, above which a bundled-nS treatment is then adopted, see figure 3.1.

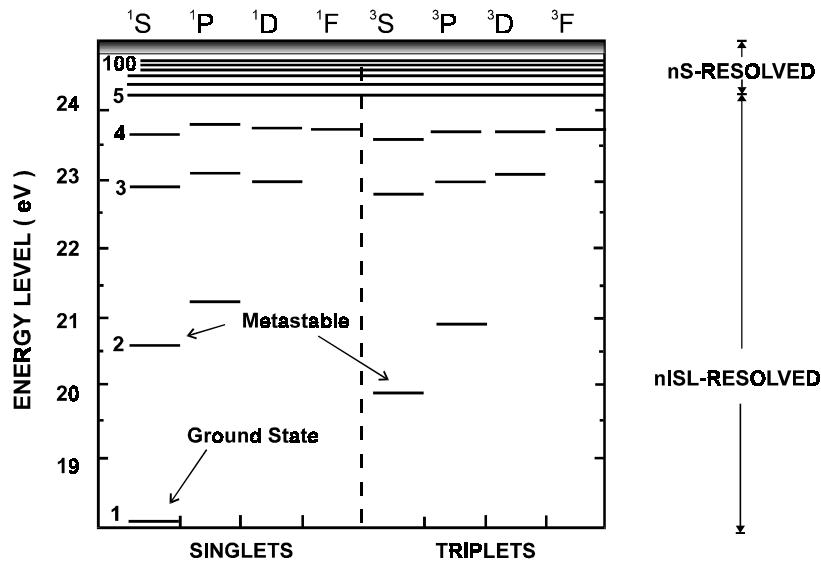


Figure 3.1 Schematic illustration of the bundled-nISL model. The low levels are calculated in an nl-resolved picture up to an arbitrary principal quantum shell, above which a bundled-nS treatment is adopted.

The switching of principal quantum numbers is such that for it and higher principal quantum shells l-redistribution is effectively complete. The ground state and the He(2 ¹S) and He(2 ³S) metastables are treated as non-equilibrium levels. Therefore the equilibrium populations of the excited states are calculated relative to each non-equilibrium level. The statistical balance equations are similar to those of the bundled-nS model but contain additional processes which were not applicable in the nS-resolved picture. These include spin changing electron collisions and collisional transitions between degenerate levels. The statistical balance equations written in matrix notation are as before,

$$v_b \frac{dN_i}{dx} = n_e n_+ \mathfrak{S}_i - \sum_j \mathcal{C}_{ij} N_j \quad 3.42$$

for $i = 1, 2, 3, \dots$

However \mathfrak{S}_i now includes recombining terms to both the singlet and the triplet excited levels and the collisional-radiative matrix is of the form,

$$\mathcal{C}_{ij} = \left[\begin{array}{c|c} \textit{Singlets} & T \rightarrow S \\ \hline S \rightarrow T & \textit{Triplets} \end{array} \right] \quad 3.43$$

where the top left hand partition concerns the atomic rates associated with the pure singlet spin system. The top right hand partition includes the atomic rates which describe the collisionally induced transitions from the triplet to singlet spin system (electron exchange collisions). The bottom right hand partition includes the atomic rates for a pure triplet spin system and the associated left hand partition contains the spin changing contribution from the singlet to the triplet spin system. The diagonal elements of the collisional-radiative matrix describes the total loss rate from each level as previously.

The approximate methods used to evaluate the cross-sections and rate coefficients in the bundled-nS model are relevant for hydrogenic and non-hydrogenic

ions in the bundled-nlSL model but require a specification of how they are to be fractionated over l-substates. In the following sub-sections we summarise the differences in the way they have been implemented. We also discuss the approximate methods employed for the atomic processes which were not applicable to the bundled-nS model. The bundled-nlSL model also accesses several databases in the same manner as the bundled-nS model, and we detail which fundamental atomic data is used. Finally, we outline the method of solving the statistical balance equations when there are three non-equilibrium levels.

3.3.1 Radiative processes

As mentioned earlier, the approximate methods employed in the bundled-nS model can be used for hydrogenic and non-hydrogenic ions in the bundled-nlSL model. Where appropriate however exact energy levels and statistical weights for helium are adopted. Exact energy levels for the low levels in the bundled-nlSL model are expanded over the complete manifold of levels using the quantum defect method for each spin system. That is the quantum defect is calculated using a series expansion.

$$\mu = a_1 + a_2 E_1 + a_3 E_2^2 + a_4 E_3^3 \quad 3.44$$

where the energy levels E_1 , E_2 and E_3 are the exact values which are entered as input. This is repeated for the s, p, and d l-series and for both spin systems with the energy levels then calculated from,

$$E_{nl} = \frac{z_0^2 I_H}{(n - \mu)^2} \quad 3.45$$

Higher l-series have negligible quantum defects. The statistical weights depend on whether we are concerned with levels which are part of the low level nlSL-resolved treatment or the high level bundled-nS picture. If we define n_2 as the arbitrary principal quantum shell which separates the nlSL and nS resolved treatment. The statistical weights are defined as,

$$n < n_2 \quad i \equiv nlSL \quad w_i = (2L + 1)(2S + 1) \quad 3.46$$

$$n > n_2 \quad i \equiv nS \quad w_i = n^2 (2L_p + 1)(2S_p + 1) \quad 3.47$$

where L_p and S_p are the total angular and spin quantum numbers associated with the parent ion. We also require nl-resolved bound-bound and bound-free Gaunt factors to evaluate quantities such as the spontaneous emission and the radiative recombination coefficient. The expressions used to evaluate these factors are of considerable complexity and a detailed account can be found in the work of Summers[43].

3.3.2 Collisional processes

The expressions which were used for the bundled-nS model form a starting point for the bundled-nlSL model. However there are several additional processes which have to be taken into account which were not applicable in the nS-resolved picture. These processes include ion and electron collisions between degenerate levels and electron driven spin changing collisions. The approximate methods to evaluate the rate coefficients for each of these processes is discussed in detail by Summers[43]. We simply quote the results here. For degenerate collisions due to electrons and ions, the rate coefficient is given as,

$$q_{nlSL \rightarrow n'l'SL'} = \sqrt{\pi} \alpha c a_0^2 \left(\frac{I_H}{kT_e} \right)^{\frac{1}{2}} \left(\frac{m}{m_e} \right)^{\frac{1}{2}} \frac{1}{z_1^2} D_{nlSL \rightarrow n'l'SL'} \left\{ 26.57 + \log \left(\frac{z_1^2 T m_e}{D_{nl} m} \right) + \log R_c^2 \right\}$$

where m and T are respectively the mass and temperature of the colliding particle. The quantity R_c^2 is described as a cut-off to ensure the collision cross sections have finite values. The expression for spin changing transitions between each spin system is,

$$q_{nlSL \rightarrow n'l'S'L'} = \frac{5}{12} \frac{(2L' + 1)(2S' + 1)}{(2L_p + 1)(2S_p + 1)} |\eta_{n'l'}^{nl}|^2 q(\epsilon_1 \rightarrow \epsilon_2) \quad S \neq S' \quad 3.48$$

where $\eta_{n'l'}^{nl}$ is an overlap fractional function. A detailed account of each expression can also be found in the work of Spence[19].

3.3.3 Fundamental atomic data

The supplementary data is stored in a similar format to the data used for the bundled-nS model. There are three databases which contain electron impact excitation, electron impact ionisation and ion-atom collision data respectively. If we first consider the electron impact excitation database. This database contains excitation rates which have been stored in the form of effective collision strengths for dipole and non-dipole transitions between all the resolved levels up to the n=4 shell. The contents of the database is primarily from the compilation of de Heer[56] but includes the work of many others[54]. Also included in this database is a compilation of spontaneous emission coefficients, the details of which can also be found in [54]. Focusing on the electron impact ionisation database. This database contains Maxwell averaged electron impact ionisation rates associated with the ground state and the He(2 ¹S) and He(2 ³S) metastables. This data is based on the work of Bell et. al.[55] and Fujimoto[57]. The ion-atom database, which is the largest database, contains cross-sections for charge exchange, ion impact excitation and ionisation from the ground and excited states of the singlet and triplet spin system. For this work the data used was based on a compilation by Summers[54].

3.3.4 Method of solution

In the same manner as the bundled-nS model, the bundled-nISL model solves for the effective contributions. As shown earlier in section 3.2.5, the quasi-static populations can be obtained using the expression,

$$N_j^{eq} = n_e n_+ R_j + n_b n_+ G_j + \sum_{\sigma=1}^m E^\sigma N_\sigma \quad 3.49$$

where in this case the number of non-equilibrium levels is three. Using the modified Saha-Boltzmann equation which is now written as,

$$N_i = n_e n_+ 8 \left(\frac{\pi a_0^2 I_H}{kT_e} \right)^{3/2} \frac{w_i}{2w_+} \exp\left(-\frac{I_i}{kT_e}\right) b_i \quad 3.50$$

where w_+ is the statistical weight of the parent ion,

$$w_+ = (2L_p + 1)(2S_p + 1) \quad 3.51$$

Equation 3.49 can be re-written in terms of the b_{nl}^{2S+1L} factors,

$$b_{nl}^{2S+1L} = FI_{(nlS)} \left(\frac{N_{1^1S}}{n_+} \right) + FII_{(nlS)} \left(\frac{N_{2^1S}}{n_+} \right) + FIII_{(nlS)} \left(\frac{N_{2^3S}}{n_+} \right) + F^2_{(nlS)} \quad 3.52$$

The quantities $FI_{(nlS)}$, $FII_{(nlS)}$ and $FIII_{(nlS)}$ separate the effective excitation contributions which populate the excited levels by driving from the ground state and the He(2^1S) and He(2^3S) metastables respectively. The contribution to populating the excited levels due to recombination from the continuum is $F^2_{(nlS)}$. It should be noted that the charge exchange $F^3_{(nlS)}$ contribution had been omitted from equation 3.52, since we have not incorporated charge exchange data for the thermal plasma atom case. The solution of equation 3.52 is achieved by a combination of switching on and off a synthetic radiation field in a similar manner as in the bundled-nS model.

The tabulated output from the model contains the excitation contributions (FI , FII , $FIII$) and the solution of the Saha-Boltzmann equation in the form $N_{nl}^{2S+1L} / b_{nl}^{2S+1L} \times n_+$. Also included are the effective cross coupling coefficients which are calculated using the expression discussed in chapter 2.0,

$$S_{\rho\sigma} = C_{\rho\sigma} - \sum_{j>m} \sum_{i>m} C_{\rho j} C_{ji}^{-1} C_{i\sigma} \quad 3.53$$

The equilibrium populations relative to the ground state and each metastable are then obtained from the tabulated output using the following relations.

$$\frac{N_{nl}^{2S+1L}}{N_{1^1S}} = FI_{(nlS)} \left(\frac{N_{nl}^{2S+1L}}{b_{nl}^{2S+1L} n_+} \right) \quad 3.54$$

$$\frac{N_{nl}^{2S+1L}}{N_{2^1S}} = FII_{(nlS)} \left(\frac{N_{nl}^{2S+1L}}{b_{nl}^{2S+1L} n_+} \right) \quad 3.55$$

$$\frac{N_{nl}^{2S+1L}}{N_{2^3S}} = FIII_{(nlS)} \left(\frac{N_{nl}^{2S+1L}}{b_{nl}^{2S+1L} n_+} \right) \quad 3.56$$

The effective beam emission coefficients relative to each metastable can then be defined in a similar manner as in section 3.2.5 .

3.4 Computational implementation and validation

3.4.1 Implementation of the models within ADAS

The bundled-nS model has been implemented into the ADAS system as ADAS310. We summarise the main features of ADAS310 here and further details can be found in [26]. As with all ADAS programs, there are three main IDL compound widgets which serve as the user interface. The input, the main processing and the output screen. We focus our attention here on the main processing screen of ADAS310, see figure 3.2.

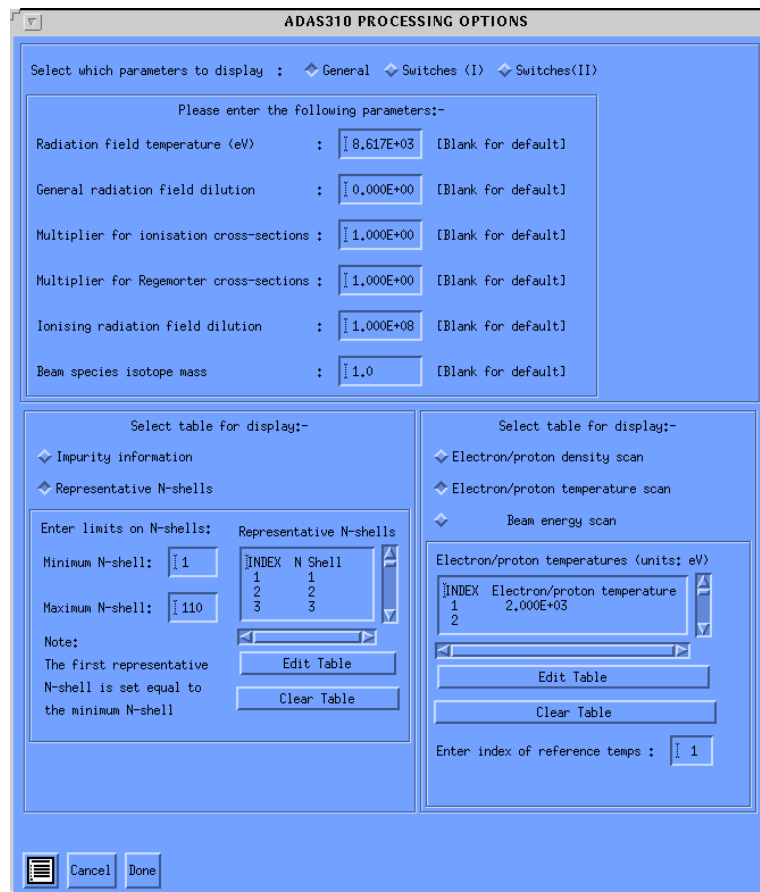


Figure 3.2 Snapshot of the main processing screen of ADAS310.

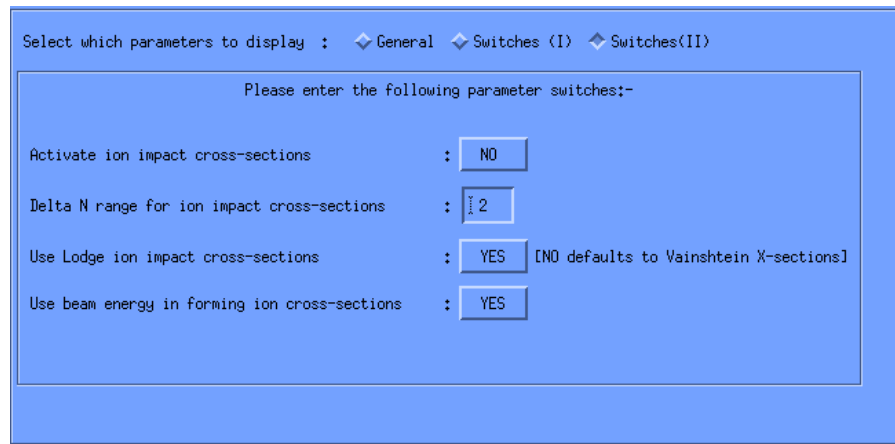
The processing screen consists of several panels which allow the user to select and enter the required input parameters. The bottom left hand panel concerns the selection of plasma impurity ions and the range of principal quantum shells for which the excited state population is to be evaluated. The panel on the bottom right allows the user to enter the required temperature, density and neutral beam energy range. The panel at the top is of most interest, since it is in this area where the user can select the different approximate methods to evaluate the rate coefficients for the atomic processes included in the statistical balance equations. As can be seen in the top panel of figure 3.2, there are a series of toggle buttons. If the user activates the button which is labelled 'Switch I', an additional panel will appear, see figure 3.3.

Figure 3.3 Snap shot of the panel which appears when the button labelled 'Switch I' is activated.

This panel allows the user to select the method for evaluating the electron impact excitation cross sections and hence the rate coefficients. The panel also contains the switch which allows the user to access the collection of fundamental atomic databases. If this switch is activated the data contained in each database is extracted and is used to replace the values obtained from the approximate methods. In the context of ADAS, each of the databases are stored in their own specific ADAS data file format (adf). The database containing electron impact excitation rates is archived in the file format known as adf04. The electron impact ionisation data is archived according to the prescription of the file format adf07, while the ion-atom

database is stored in the file format of adf02. A detail description of each of the file formats can also be found in [26].

If the user now activates the button labelled ‘switch II’, a second panel will appear, see figure 3.4.



The screenshot shows a software interface with a blue background. At the top, it says "Select which parameters to display : General Switches (I) Switches(II)". Below this is a box containing the text "Please enter the following parameter switches:-". There are four rows of controls:

Activate ion impact cross-sections	:	<input type="button" value="NO"/>	
Delta N range for ion impact cross-sections	:	<input type="text" value="2"/>	
Use Lodge ion impact cross-sections	:	<input type="button" value="YES"/>	[NO defaults to Vainshtein X-sections]
Use beam energy in forming ion cross-sections	:	<input type="button" value="YES"/>	

Figure 3.4 Snapshot of the panel which appears when the button labelled ‘Switch II’ is activated.

This panel allows the user to choose between the different approximate methods which are employed to evaluate ion impact excitation cross-sections. The panel also contains switches which allow the user to turn off the ion collisions as well as to form the ion-atom rate coefficients without taking into account the beam velocity. The latter being equivalent to switching the beam off and modelling the excited state population structure of deuterium in a thermal plasma.

After the user has finalised their selection, ADAS310 then loops around the specified range of temperatures, densities and neutral beam energies. In each case assembling the statistical balance equations and solving for the equilibrium populations and effective beam stopping coefficients. The main output, which is in the ADAS adf26 type format, contains tables of the F 's, b_n 's and the effective beam stopping coefficients. We show in table 3.1 the typical output from ADAS310 for a relatively simple case.

TABLE FOR ION PRINCIPAL QUANTUM SHELL POPULATIONS IN THERMAL PLASMA						
		Z0 = 1.00E+00	Z1 = 1.00E+00			
TRAD = 1.00E+08 K		TE = 2.32E+07 K		TP = 2.32E+07 K		
W = 0.00E+00		NE = 1.00E+12 CM-3		NP = 1.00E+12 CM-3		
EH = 5.00E+03 EV/AMU		NH = 1.00E+07 CM-3		NH/NE = 1.00E-05 FLUX = 9.78E+14 CM-2 SEC-1		
CX OFF : N1/N+ = 1.16108E-09 RECOMB COEFF = 1.42279E-16 CM+3 SEC-1 IONIZ COEFF = 1.22541E-07 CM+3 SEC-1						
CX ON : N1/N+ = 4.76864E-05 RECOMB COEFF = 5.84353E-12 CM+3 SEC-1 IONIZ COEFF = 1.22541E-07 CM+3 SEC-1						
I	N	F1	F2	F3	B(CHECK)	B(ACTUAL) NN/(BN*N+)
1	1	0.00000E+00	3.11171E+05	1.27797E+15	1.27804E+10	1.27804E+10 3.73131E-15
2	2	3.60194E+09	3.49143E+00	7.13883E+10	8.85650E+05	8.85650E+05 1.48493E-14
3	3	1.27748E+09	2.34706E+00	4.34908E+10	4.95829E+05	4.95829E+05 3.33793E-14
4	4	5.08493E+08	1.60159E+00	5.95132E+09	8.37630E+04	8.37630E+04 5.93213E-14
5	5	1.36343E+08	1.17348E+00	8.63307E+08	1.51359E+04	1.51359E+04 9.26753E-14
6	6	3.94663E+07	1.05453E+00	1.63609E+08	3.51915E+03	3.51915E+03 1.33441E-13
7	7	1.40732E+07	1.01994E+00	4.03570E+07	1.07569E+03	1.07569E+03 1.81619E-13
8	8	5.82632E+06	1.00836E+00	1.22062E+07	4.00906E+02	4.00906E+02 2.37209E-13
9	9	2.80157E+06	1.00404E+00	4.43355E+06	1.78936E+02	1.78936E+02 3.00211E-13
10	10	1.61959E+06	1.00234E+00	1.97951E+06	9.80297E+01	9.80297E+01 3.70626E-13
11	11	1.23372E+06	1.00178E+00	1.21778E+06	7.20110E+01	7.20110E+01 4.48452E-13
12	12	8.60349E+05	1.00124E+00	7.15872E+05	4.91869E+01	4.91869E+01 5.33690E-13
13	15	2.76860E+05	1.00040E+00	1.61784E+05	1.58207E+01	1.58207E+01 8.33876E-13
14	20	5.23029E+04	1.00007E+00	2.37014E+04	3.73122E+00	3.73122E+00 1.48243E-12
15	30	6.82995E+03	1.00001E+00	2.84341E+03	1.35414E+00	1.35414E+00 3.33543E-12
16	40	1.54437E+03	1.00000E+00	6.25293E+02	1.07990E+00	1.07990E+00 5.92963E-12
17	50	4.75304E+02	1.00000E+00	1.89911E+02	1.02457E+00	1.02457E+00 9.26503E-12
18	60	1.75921E+02	1.00000E+00	6.97467E+01	1.00909E+00	1.00909E+00 1.33416E-11
19	70	7.19489E+01	1.00000E+00	2.83621E+01	1.00371E+00	1.00371E+00 1.81594E-11
20	80	2.98631E+01	1.00000E+00	1.16986E+01	1.00154E+00	1.00154E+00 2.37184E-11
21	90	1.07568E+01	1.00000E+00	4.16035E+00	1.00055E+00	1.00055E+00 3.00186E-11
22	100	1.27021E+00	1.00000E+00	4.26867E-01	1.00006E+00	1.00006E+00 3.70601E-11
BN = F1*(N1/N+) + F2 + F3*(NH/NE)						
N1 = POPULATION OF GROUND STATE OF ION						
N+ = POPULATION OF GROUND STATE OF NEXT IONISATION STAGE						
NN = POPULATION OF PRINCIPAL QUANTUM SHELL N OF ION						
BN = SAHA-BOLTZMANN FACTOR FOR PRINCIPAL QUANTUM SHELL N						
EH = NEUTRAL HYDROGEN BEAM ENERGY						
W = RADIATION DILUTION FACTOR						
Z0 = NUCLEAR CHARGE						
Z1 = ION CHARGE+1						
NIP = 0 INTD = 3 IPRS = 1 ILOW = 1 IONIP = 1 NIONIP = 2 ILPRS = 1 IVDISP = 1						
ZEFF = 1.0 TS = 1.00D+08 W = 0.00D+00 CION = 1.0 CPY = 1.0 W1 = 1.00D+08 ZIMP = .0(0.00D+00)						
1						

Table 3.1 Typical output from ADAS310 for a pure D⁺ plasma. The output from ADAS310 is archived according to the file format of adf26. A summary of the input parameters is specified at the bottom of the tabulated output.

It is common practice to generate effective stopping and emission coefficients for a wide range of plasma parameters. The plasma parameters being the temperature, density and neutral beam energy. The typical output from ADAS310 for a single impurity species is approximately 3.5 Mb and consists of a series of tables as shown in table 3.1. We then have to extract the effective stopping and emission coefficients and store them in a suitable format. To automate this process, during the course of this work we have developed an interactive program which is employed to

interrogate the adf26 type files. The program offers the user the choice of whether to extract effective stopping or effective emission coefficients for an arbitrary transition from the adf26 type file. This program is known as ADAS312 and we summarise the main features here, a more detailed description can be found in [58]. We show in figure 3.5 the main processing screen of ADAS312.

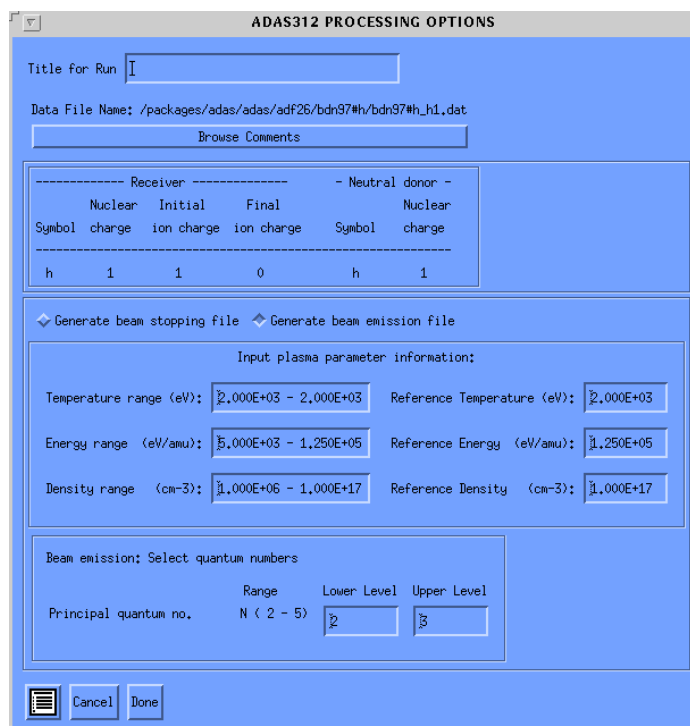


Figure 3.5 Snap shot of the main processing screen of ADAS312.

The processing screen consist of several panels. The panel in the middle displays the parameter range over which the contents of the adf26 type file has been evaluated. It is also within this panel that the user selects whether effective stopping or emission coefficients are to be extracted from the adf26 type file. If the user activates the beam emission button, the panel at the bottom is sensitised. This panel allows the user to enter the upper and lower principal quantum number for the transition corresponding to the effective beam emission coefficient which is required. If the user activates the beam stopping button, the bottom panel is de-sensitised which prevents the user entering any information. Once the user has finalised their selection and activated the button labelled ‘Done’, the user is presented with the output screen. This screen offers several choices, the user can choose to save the extracted data to file or to

view the data as a surface plot or even both. If we consider the scenario where both of the options have been selected. The user is then presented with a graphical screen which contains a surface plot of the selected data, see figure 3.6.

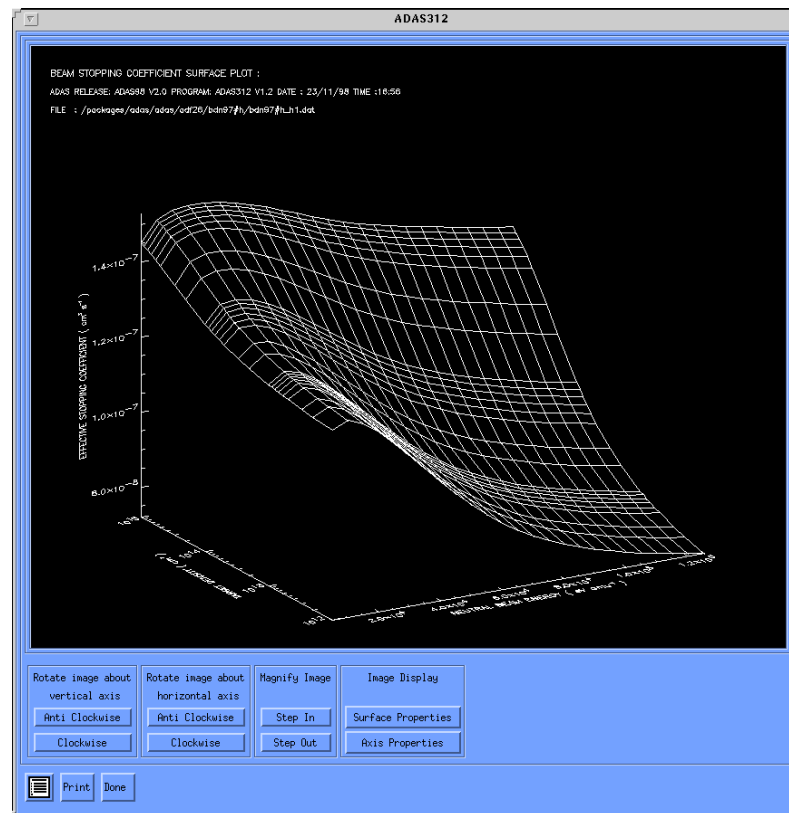


Figure 3.6 Snapshot of the graphical screen of ADAS312.

The graphical screen allows the user to interactively inspect the data by being able to zoom in or out or by rotating the surface plot through various angles. If the user activates the ‘print’ button the contents of the graphics window will then be written to an appropriate graphics file. Once the user returns back to the output screen by activating the ‘done’ button, the selected data is then written to file. The effective stopping and emission coefficients are respectively archived according to the specifications of the ADAS adf21 and adf22 type files. We show in table 3.2 an example of an adf21 type file which contains effective stopping coefficients for a pure D^+ plasma.

```

1 /SCREF=1.081E-07 /SPEC=H /DATE=09/04/98 /CODE=ADAS312
-----
25 25 /TREF=2.000E+03
-----
5.000E+03 1.000E+04 1.500E+04 2.000E+04 2.500E+04 3.000E+04 3.500E+04 4.000E+04
4.500E+04 5.000E+04 5.500E+04 6.000E+04 6.500E+04 7.000E+04 7.500E+04 8.000E+04
8.500E+04 9.000E+04 9.500E+04 1.000E+05 1.050E+05 1.100E+05 1.150E+05 1.200E+05
1.250E+05
1.000E+12 2.000E+12 3.000E+12 5.000E+12 6.000E+12 7.000E+12 8.000E+12 9.000E+12
1.000E+13 2.000E+13 3.000E+13 5.000E+13 6.000E+13 7.000E+13 8.000E+13 9.000E+13
1.000E+14 2.000E+14 3.000E+14 5.000E+14 6.000E+14 7.000E+14 8.000E+14 9.000E+14
1.000E+15
-----
1.225E-07 1.246E-07 1.229E-07 1.198E-07 1.160E-07 1.120E-07 1.079E-07 1.038E-07
9.981E-08 9.607E-08 9.272E-08 8.966E-08 8.704E-08 8.473E-08 8.274E-08 8.104E-08
7.953E-08 7.823E-08 7.706E-08 7.601E-08 7.506E-08 7.418E-08 7.338E-08 7.264E-08
7.195E-08
. . . . .
. . . . .
. . . . .
. . . . .
1.450E-07 1.505E-07 1.523E-07 1.529E-07 1.528E-07 1.523E-07 1.514E-07 1.502E-07
1.488E-07 1.472E-07 1.456E-07 1.439E-07 1.425E-07 1.411E-07 1.399E-07 1.388E-07
1.378E-07 1.369E-07 1.361E-07 1.353E-07 1.345E-07 1.337E-07 1.330E-07 1.323E-07
1.316E-07
-----
20 /EREF=6.500E+04 /NREF=6.000E+13
-----
1.000E+02 2.000E+02 3.000E+02 5.000E+02 6.000E+02 7.000E+02 8.000E+02 8.966E+02
1.000E+03 2.000E+03 3.000E+03 5.000E+03 6.000E+03 7.000E+03 8.000E+03 8.966E+03
1.000E+04 2.000E+04 3.000E+04 5.000E+04
-----
1.302E-07 1.294E-07 1.268E-07 1.222E-07 1.203E-07 1.187E-07 1.173E-07 1.161E-07
1.150E-07 1.081E-07 1.045E-07 1.003E-07 9.883E-08 9.763E-08 9.659E-08 9.570E-08
9.484E-08 8.903E-08 8.517E-08 7.971E-08
-----
C
C
C ADAS FILE TYPE : ADF21
C SOURCE FILE : /packages/adas/adas/adf26/bdn97#h/bdn97#h_h1.dat
C
C USER ID : anderson
C
-----

```

Table 3.2 Example of an adf21 type file which contains effective stopping coefficients for a pure D⁺ plasma.

The format of the adf22 type files are identical to the structure shown in table 3.2 but contain effective emission coefficients. In both of the file formats, the effective coefficients are stored as a one and two dimensional grids tuned for rapid experimental analysis, see chapter 4.0.

The bundled-nlSL model is intended to be placed into the ADAS system as ADAS311 in the near future. At the moment it is an off line program which is driven by an ASCII file containing all the relevant input parameters. The output file from the program, which is also classified as an ADAS adf26 type file, contains the F's and

the b-factors for both the singlet and triplet spin system. The collisional-radiative cross coupling coefficients are also included. We show in table 3.3 the typical output from ADAS311.

EFFECTIVE CONTRIBUTION TABLE FOR ION PRINCIPAL QUANTUM SHELL POPULATIONS IN THERMAL PLASMA											
HELIUM		Z0 = 2.00E+00	Z1 = 1.00E+00								
TRAD = 1.00E+08 K		TE = 1.16E+06 K		TP = 1.16E+06 K							
W = 0.00E+00		NE = 1.00E+05 CM-3		NP = 1.00E+00 CM-3							
EH = 1.00E+00 EV/AMU		NH = 1.00E+07 CM-3		NH/NE = 1.00E+02		FLUX = 1.38E+13 CM-2 SEC-1					
COLLISIONAL DIELECTRONIC RATES											
EFFECTIVE IONISATION AND CROSS COUPLING RATES											
IG	I	ALF	1		2		31				
1	1	2.1711471E-13	2.1383283E-08	-1.8729842E-06	-2.7239829E-09						
2	2	7.9081675E-15	-8.5961126E-10	2.0900639E-06	-6.5498303E-10						
3	31	6.4304632E-13	-5.0658281E-10	-1.9117015E-08	2.0775860E-07						
LEVELS OF MULTIPLICITY 1											
0	IR	N	L	LT	F1(I)	F1(II)	F1(III)	F2	B(CHECK)	B(ACTUAL)	NL/(B*N+)
1	1	0	0		9.4362731E+19	0.0000000E+00	0.0000000E+00	0.0000000E+00	1.0737047E+15	1.0737047E+15	1.0597404E-20
2	2	0	0		0.0000000E+00	1.1597567E+20	0.0000000E+00	0.0000000E+00	1.0950908E+12	1.0950908E+12	8.6224984E-21
3	2	1	1		1.2865979E+07	3.7700009E+09	5.5303704E+06	1.2068034E+02	3.1994921E+02	3.1994921E+02	2.5712114E-20
4	3	0	0		1.0193884E+08	1.6740420E+10	3.6584276E+07	2.1798098E+03	3.6120702E+03	3.6120702E+03	8.4259830E-21
5	3	1	1		9.5648714E+06	4.2821961E+08	4.8132494E+05	1.0442881E+02	2.1880951E+02	2.1880951E+02	2.5235828E-20
.
.
.
30	100	0	0		9.2732992E+03	1.2002970E+05	4.5014386E-05	4.4865574E+00	4.5932069E+00	4.5932069E+00	8.2867359E-17
LEVELS OF MULTIPLICITY 3											
0	IR	N	L	LT	F1(I)	F1(II)	F1(III)	F2	B(CHECK)	B(ACTUAL)	NL/(B*N+)
31	2	0	0		0.0000000E+00	0.0000000E+00	3.8351874E+19	0.0000000E+00	1.1980260E+14	1.1980260E+14	2.6074345E-20
32	2	1	1		3.6114582E+07	2.1225959E+09	1.3754551E+11	5.2880585E+04	4.8297269E+05	4.8297269E+05	7.7332539E-20
.
.
.
57	80	0	0		3.5531061E-05	6.1125850E-04	2.0290738E+05	1.9135280E+01	1.9769117E+01	1.9769117E+01	1.5910655E-16
58	90	0	0		1.1637887E-05	2.1689818E-04	8.9550399E+04	8.9357444E+00	9.2154797E+00	9.2154797E+00	2.0136833E-16
59	100	0	0		3.2309871E-06	7.0890962E-05	3.9861521E+04	4.4877036E+00	4.6122220E+00	4.6122220E+00	2.4860208E-16
B = F1(I)*(N1/N+) F1(II)*(N2/N+) +F1(III)*(N3/N+) +F2 N1 = POPULATION OF THE 1s2 1S METASTABLE N2 = POPULATION OF THE 2s 1S METASTABLE N3 = POPULATION OF THE 2s 3S METASTABLE N+ = POPULATION OF GROUND STATE OF NEXT IONISATION STAGE NL = POPULATION OF RESOLVED NL QUANTUM SHELL OF ION B = SAHA-BOLTZMANN FACTOR FOR RESOLVED NL QUANTUM SHELL EH = NEUTRAL HELIUM BEAM ENERGY W = RADIATION DILUTION FACTOR Z0 = NUCLEAR CHARGE Z1 = ION CHARGE+1											
NIP = 2 INTD = 3 IPRS = 1 ILOW = 1 IONIP = 1 NIONIP = 2 ILPRS = 1 IVDISP = 1 ZEFF = 4.0 TS = 1.00D+08 W = 0.00D+00 CION = 0.0 CPY = 0.0 W1 = 0.00D+00 ZIMP = 4.0 (2.50D+04)											

Table 3.3 Typical output from the Bundled-nISL model. The first half concerns the singlet spin system while the remainder deals with the triplet spin system. At the bottom of the tabulated data a summary of the input parameters is given.

In a similar manner as with ADAS310, we evaluate the effective cross coupling and emission coefficients over a wide range of plasma parameters. The typical output for a single plasma impurity is around 7.0 Mb. To assist in archiving and extracting the

effective coefficients from the adf26 type files, we have also developed an interactive program specifically for this task. The program is called ADAS313 and we show in figure 3.7 the main processing screen.

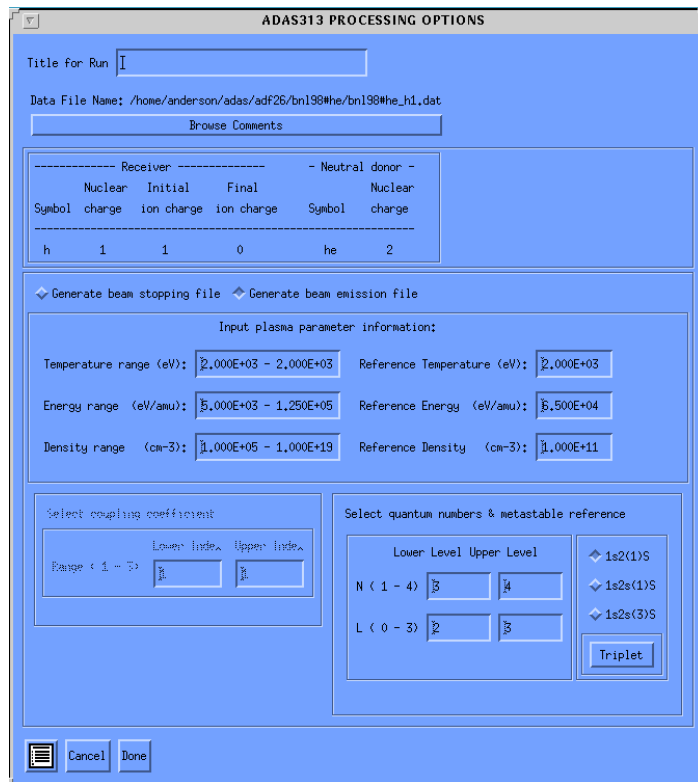


Figure 3.7 Snapshot of the main processing screen of ADAS313.

A series of panels allows the user to interactively select and enter their choices. The panel in the middle displays the parameter range over which the contents of the adf26 type file has been evaluated. This panel also houses two toggle buttons which allows the user to select between extracting effective cross coupling or emission coefficients from the adf26 type file. If the user activates the cross coupling button, the bottom left hand panel is sensitised which allows the user to specify what cross coupling coefficient is required. The coupling coefficients are specified according to the index notation of equation 3.53. If the user activates the beam emission button, the panel on the bottom right hand side is now sensitised. This panel allows the user to specify the quantum numbers according to the transition of interest. Also since the equilibrium populations are calculated relative to the ground state and the two metastables. The user also has to enter the non-equilibrium reference. Once the user

has completed their selection and activated the ‘Done’ button, a similar output screen as in ADAS312 appears. The user is then presented with the choice of either writing the effective coefficients to a file or to view the data via a surface plot or in fact both. The surface plot is generated using the same graphical window as shown for ADAS312. The effective coupling coefficients are archived as adf21 type files, while the effective emission coefficients are stored as adf22 type files.

3.4.2 Validation of ADAS310, the bundled-nS model

As discussed earlier the collisional-radiative ionisation coefficients, which are calculated by ADAS310, represents the rate at which the beam neutrals are ionised as the beam penetrates into the plasma. This rate of ionisation is determined by the outcome of the competing collisional and radiative processes which in turn are governed by the plasma density. In the case of a low density plasma where collisional excitation is balanced by spontaneous emission. The only processes which contribute to the ionisation of the beam neutrals are direct process from the ground state via charge exchange and impact ionisation. Therefore the low density ionisation rate is simply the sum of these direct rate coefficients. This low density ionisation rate was compared with the ionisation coefficient calculated by ADAS310 in the low density regime. A similar approach was applied to a high density plasma. In a high density plasma the rate at which the beam neutrals are ionised is simply the sum of the collisional excitation and ionisation coefficients from the ground state of the neutrals. A variety of composite target plasmas were considered. As an example we show in figure 3.8 the results for both a pure D^+ and C^{6+} plasma.

If we confine ourselves with the asymptotic limits of the stopping coefficient for a pure D^+ plasma. It can be observed that in the low density regime the results from ADAS310 and the theoretically predicted values agree exactly. In the high density limit a maximum difference of 1.92 % can be seen. If we now consider the plot on the right in figure 3.8 which illustrates the asymptotic limits for a pure C^{6+} plasma. In the low density limit the results between ADAS310 and theory agree exactly and in the high density regime a maximum difference of 4.13 % can be observed. This difference arise due to the fact that the theoretical values have been evaluated using the rate coefficients for the atomic processes only up to the $n=4$ shell.

If we were to include more atomic processes while evaluating the theoretical limits the difference would tend to zero.

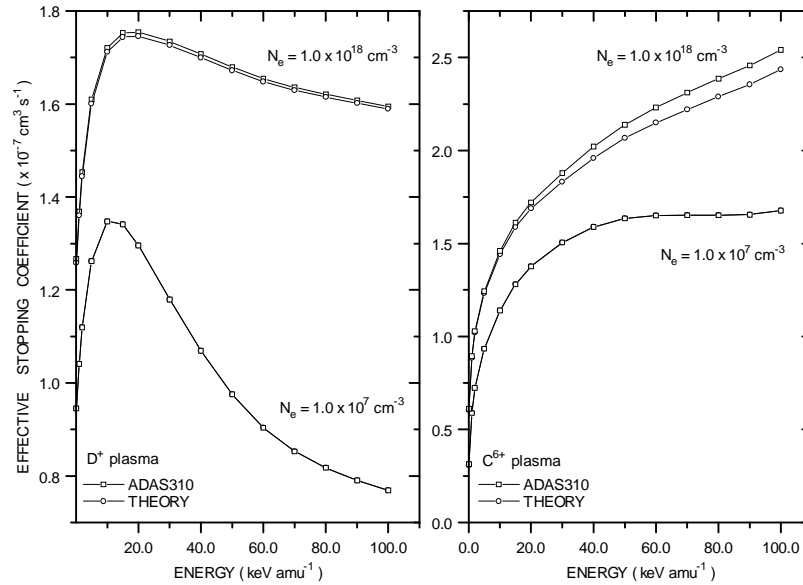


Figure 3.8 Comparison between the results of ADAS310 and the theoretical predictions of the asymptotic limits of the stopping coefficient. The plot on the left shows the results in the low and high density limit for a pure D^+ plasma. Similar results are shown for a pure C^{6+} plasma in the plot on the right. The low and high density limit respectively correspond to an electron density of 1.0×10^7 and $1.0 \times 10^{18} \text{ cm}^{-3}$. At $1.0 \times 10^7 \text{ cm}^{-3}$ the low density limit and ADAS310 for a D^+ plasma are superimposed. The plasma temperature was $1.0 \times 10^3 \text{ eV}$

We then went on to ensure that the excited state population were being evaluated correctly. To achieve this we compared the excited state population structure of ADAS310 with an independent low level population code ADAS205[26]. ADAS205 calculates the excited population structure of neutral deuterium, ignoring higher levels, in a thermal plasma. It was necessary to define a set of low levels in ADAS310 to simulate the same conditions as in ADAS205. It should also be noted that ADAS205 only includes electron collisions, therefore it was necessary to suppress any ion collisions in ADAS310. We found that the excited state populations were in agreement.

3.4.3 Validation of ADAS311, the bundled-nlSL model

To validate ADAS311 a similar approach was adopted. However while investigating the asymptotic limits of the effective coupling coefficient we ran the program with only the ground state specified as the non-equilibrium level. This enable us to be able to focus on one effective coefficient. We found that it agreed with the value predicted by summing the appropriate rate coefficients. We then compared the populations obtained from ADAS208[26] to that of ADAS311. ADAS208 calculates the excited population structure of an arbitrary ion in an nl-resolved picture and is a more advance version of ADAS205. To ensure the comparison was equivalent a similar set of representative levels were selected. For a wide range of plasma parameters we found that there was excellent agreement. As an example we show the equilibrium populations for the first few levels calculated by ADAS311 and ADAS208 for a pure D^+ plasma.

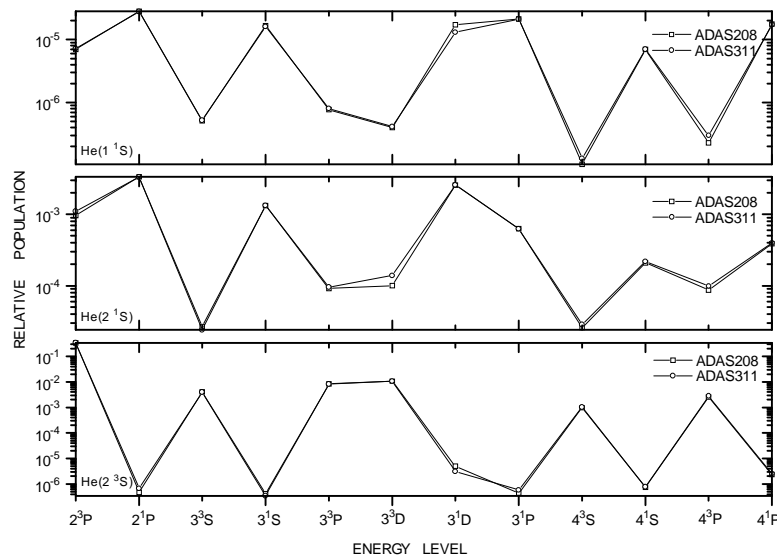


Figure 3.9 Comparison between the excited population structure calculated using ADAS208 and ADAS311. Working downwards, the population of each levels are calculated relative to the He(1 1S) ground state and the two metastables, He(2 1S) and He(2 3S). The electron density and the plasma temperature was respectively $1.0 \times 10^{13} \text{ cm}^{-3}$ and $2.0 \times 10^3 \text{ eV}$.

3.5 Summary

We have described the formulation and implementation of the bundled-nS and bundled-nlSL model. The bundled-nS model is employed to calculate the attenuation and excited population structure of neutral deuterium beam atoms, while the bundled-nlSL model is employed to calculate the attenuation and excited population structure of neutral helium beam atoms.

The bundled-nS model in the context of ADAS is known as ADAS310. During the course of this work we have developed an interactive program which interrogates the output from ADAS310. This program is called ADAS312 and its role is to extract and archive effective beam stopping and emission coefficients in their respective formats of adf21 and adf22.

The Bundled-nlSL model, which has also been developed during the course of this work, is intended to be placed into the ADAS packaged as ADAS311. At the moment it is an off line program which is driven by an ASCII file containing the appropriate input parameters. The output of ADAS311 is also interrogated by a new post processing program which is called ADAS313. ADAS313 extracts cross coupling and effective emission coefficients which are respectively stored in their ADAS data formats of adf21 and adf22.